Compressive Sensing and Generalized Likelihood Ratio Test in SAR Tomography

G. Fornaro[1,2], A. Pauciullo[1], D. Reale[1], M. Weiss[3], A. Budillon[2], G. Schirinzi[2]

1 - Institute for Electromagnetic Sensing of the Environment (IREA)
National Research Council (CNR), Naples, Italy

2 - University of Napoli "Parthenope"
Department of Engineering, Naples, Italy

3- Fraunhofer FHR
Wachtberg, Germany.



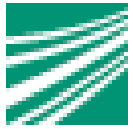

Outline

- Synthetic Aperture Radar (SAR) Tomography and motivation for super-resolution
- Compressive Sensing in Tomo-SAR
- Scatterer detection problem Tomo-SAR . Generalized Likelihood Ratio Test (GLRT) schemes: the GLRT with cancellation (GLRT-C) and the support based GLRT (sup-GLRT) approaches
- Application to real data: CS, GLRT-C vs sup-GLRT and sup-GLR vs CS
- Conclusions and future works

SAR Tomography for full 3D Imaging

- SAR Interferometry and Differential SAR Interferometry has important applications in Digital Elevation Model (DEM) reconstruction and monitoring of deformation.
- SAR Tomography extends interferometric approaches for application to complex scenarios.
- By **synthesizing an antenna also in the slant height** direction (orthogonal to the line of sight) it is possible to analyze the **vertical structure of the** scattering thus extending SAR imaging **form 2D** (azimuth-slant range) **to 3D** (azimuth-slant range-slant height).

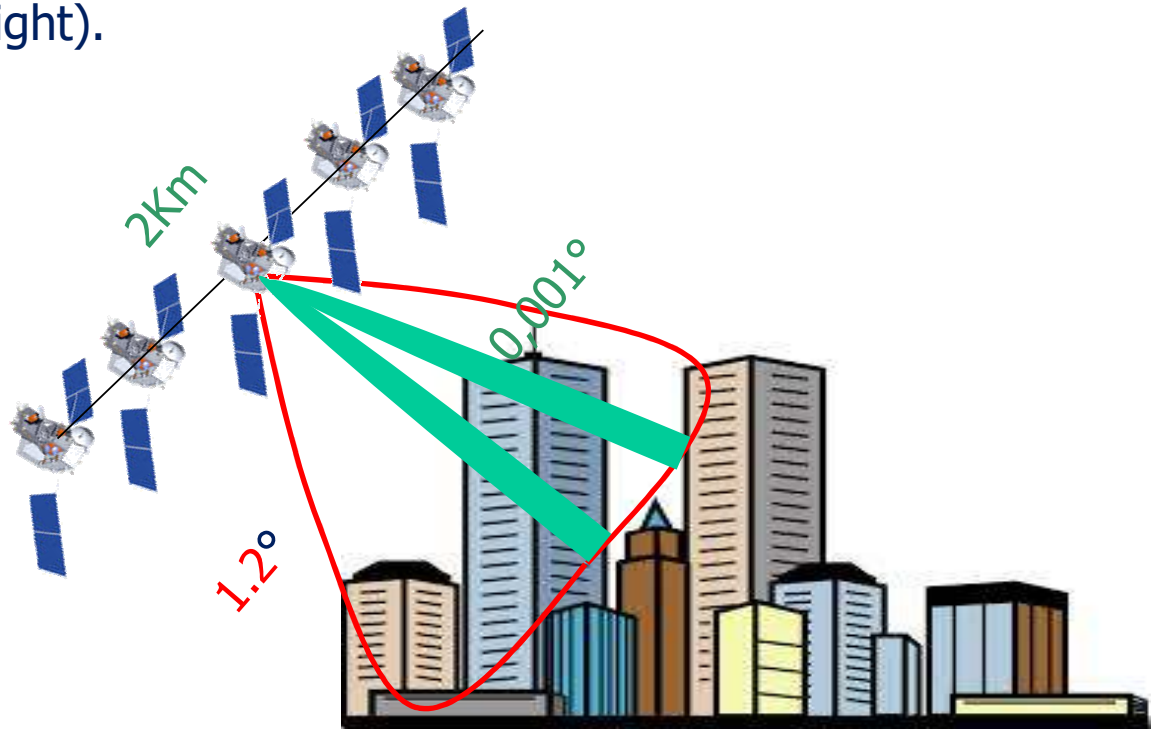

3D SAR Imaging

N acquisitions with spatial (orthogonal) baseline distribution $b_1 \ldots\ldots b_N$

backscattering distribution along the slant height

$$x_n = \int_{-s_{\max}}^{s_{\max}} \gamma(s) e^{-j2\pi\xi_n s} ds \qquad \xi_n = 2b_n/(\lambda r) \qquad n = 1,\ldots.N$$

signal to the *n*-th antenna

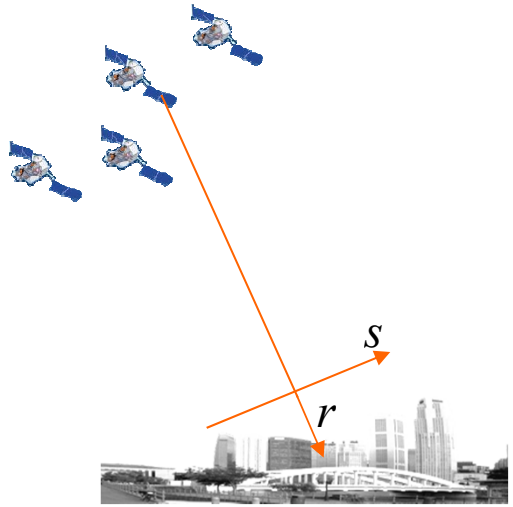

RAYLEIGH RESOLUTION

$$\Delta s = \lambda r/(2B)$$

$$B = b_{\max} - b_{\min}$$

FOURIER INVERSION FROM IRREGULAR SAMPLES:

- BeamForming (BF)
- Regularized inversion (SVD)
- Adaptive Beamforming (Capon)
- **Compressive sensing (CS)[1,2]**

1. A. Budillon, A. Evangelista, G. Schirinzi. Three-Dimensional SAR Focusing From Multipass Signals Using Compressive Sampling. IEEE Trans. Geosci. Remote Sens., 49 (1):488-499, 2011
2. X. X. Zhu, and R. Bamler. Tomographic SAR Inversion by L1 -Norm Regularization—The Compressive Sensing Approach. IEEE Trans. Geosci. Remote Sens., 48(10):3839-3846, 2010.

Beamforming – Matched filter

$$x_n = N^{-1/2} \int \gamma(s) \exp[-j2\pi\xi_n s] ds$$

$$\mathbf{x}^{\mathrm{T}} = [x_1 .... x_N] \quad N \text{ measurements}$$

DISCRETIZATION

$s \in \{s_1, ..., s_l, .., s_L\}$ L (bins): $L \geq N$ typically $L >> N$

$$\mathbf{x} = \frac{1}{\sqrt{N}} \begin{bmatrix} 1 & & 1 \\ & & \\ e^{-j2\pi\zeta_N s_1} & & e^{-j2\pi\zeta_N s_L} \end{bmatrix} \boldsymbol{\gamma} = \mathbf{A}\boldsymbol{\gamma}$$

$$\mathbf{A} = [\mathbf{a}_1 \quad ... \quad \mathbf{a}_L]$$ **sensing matrix**

$$\mathbf{a}_l^{\mathrm{T}} = \left[1 \quad ... \quad e^{-j2\pi\xi_N s_l}\right] / \sqrt{N}$$ **steering vector:** response or "firm" of a scatterer at a given height

INVERSION

$$\hat{\boldsymbol{\gamma}} = \mathbf{A}^{\mathrm{H}}\mathbf{x} \quad \Rightarrow \hat{\gamma}(s_m) = \mathbf{a}_m^{\mathrm{H}}\mathbf{x}$$

4D SAR Imaging (Differential SAR Tomography)

N acquisitions with spatial baseline distribution $b_1 \ldots\ldots b_N$ and temporal distribution $t_1 \ldots\ldots t_N$

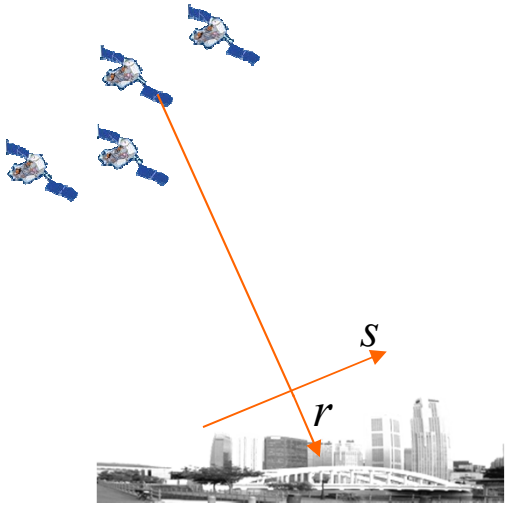

Deformation term

$$x_n = \int_{-s_{\max}}^{s_{\max}} \gamma(s) e^{-j2\pi\xi_n s} e^{-j\frac{4\pi}{\lambda} d(s,t_n)} ds$$

Signal to the *n*-th antenna

$$e^{-j\frac{4\pi}{\lambda} d(s,t_n)} = \int_{-v_{\max}}^{v_{\max}} a(s,v) e^{-j2\pi\eta_n v} dv$$

$$\eta_n = 2t_n/\lambda$$

$$x_n = \int_{-s_{\max}}^{s_{\max}} \int_{-v_{\max}}^{v_{\max}} a_\gamma(s,v) e^{-j2\pi\xi_n s - j2\pi\eta_n v} dv ds$$

$$\eta_n = 2t_n/\lambda \qquad \xi_n = 2b_n/(\lambda r)$$

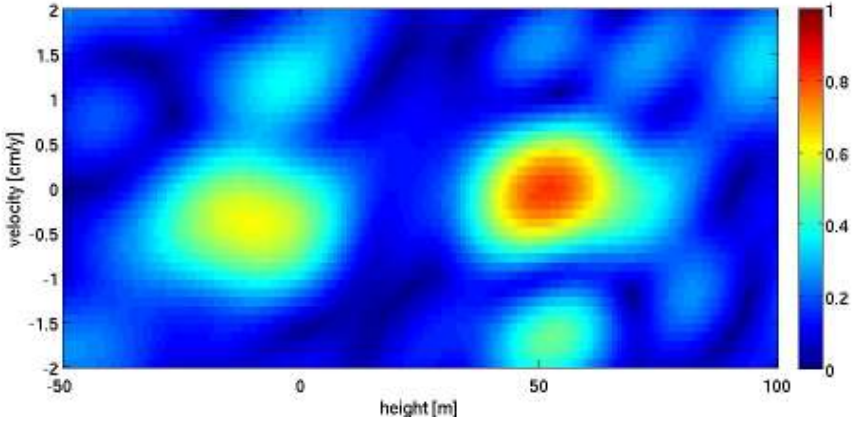

Compressive Sensing

$$\mathbf{x} = \mathbf{A}\boldsymbol{\gamma} = \begin{bmatrix} \mathbf{a}_1 & \dots & \mathbf{a}_L \end{bmatrix} \boldsymbol{\gamma} \qquad \mathbf{a}_l^{\mathrm{T}} = \begin{bmatrix} 1 & \dots & e^{-j2\pi\zeta_N s_l} \end{bmatrix} \Big/ \sqrt{N}$$

Result: if $\boldsymbol{\gamma}$ is a sparse signal (can be well represented as few non zero contributions) then, under the condition that a sufficient number of samples are acquired, the unknown can be well reconstructed via the compressive sensing technique.

$L >> N$ i.e. few measurements (N) and many unknown (L)

Hypothesis: the number K of non-zero entries of $\boldsymbol{\gamma}$ ($\|\boldsymbol{\gamma}\|_0 = K$) is sufficiently smaller than L,N ($K<<N<<L$)

$$\hat{\boldsymbol{\gamma}} = \arg\min_{\boldsymbol{\gamma}} \|\boldsymbol{\gamma}\|_0 \quad \text{subject to} \quad \|\mathbf{x} - \mathbf{A}\boldsymbol{\gamma}\|_2 < \varepsilon$$

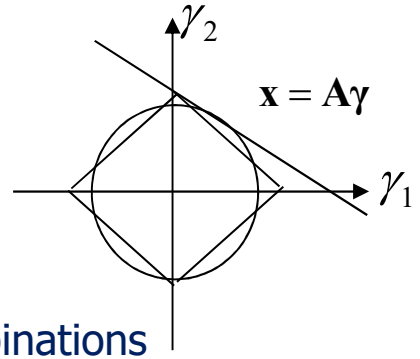

NP Complete problem, i.e. requires the check of all $L!/K!/(L\text{-}K)!$ combinations

Under "some" mild hypothesis the solution above is equal to that of one of the following (equivalent) convex problems:

$$\hat{\boldsymbol{\gamma}} = \arg\min_{\boldsymbol{\gamma}} \|\boldsymbol{\gamma}\|_1 \quad \text{subject to} \quad \|\mathbf{x} - \mathbf{A}\boldsymbol{\gamma}\|_2 < \varepsilon \qquad \hat{\boldsymbol{\gamma}} = \arg\min_{\boldsymbol{\gamma}} \left\{ \|\mathbf{x} - \mathbf{A}\boldsymbol{\gamma}\|_2 + \delta \|\boldsymbol{\gamma}\|_1 \right\}$$

Basis Pursuit De-Noising (BPDN)

Scatterer Detection Problem

Key elements: the False Alarm Probability (FAP) and the Detection Probability (DP).

$$\mathcal{H}_0: \quad \mathbf{x} = \mathbf{w}$$

$$\mathcal{H}_1: \quad \mathbf{x} = \mathbf{a}_1\gamma_1 + \mathbf{w}$$

$$\mathcal{H}_2: \quad \mathbf{x} = \mathbf{a}_1\gamma_1 + \mathbf{a}_2\gamma_2 + \mathbf{w}$$

$\gamma_1; \gamma_2$ are the scatterers' reflectivities

$\mathbf{w}$ is the additive noise

Generalized Likelihood Ratio Test (GLRT) is required.

Letting $\mathbf{p}$ to collect the unknown parameters (height, height/velocity, …) for a Gaussian model the **discrimination between the first two hypotheses** is achieved as:

$$\frac{\max_{\mathbf{p}}\left|\mathbf{a}^{\mathrm{H}}(\mathbf{p})\mathbf{x}\right|^2}{\|\mathbf{a}\|^2\|\mathbf{x}\|^2} = \frac{\max_{\mathbf{p}}\left|\mathbf{a}^{\mathrm{H}}(\mathbf{p})\mathbf{x}\right|^2}{\|\mathbf{x}\|^2} = \frac{\max_{\mathbf{p}}\left|\mathbf{x}^{\mathrm{H}}\mathbf{a}(\mathbf{p})\mathbf{a}^{\mathrm{H}}(\mathbf{p})\mathbf{x}\right|^2}{\|\mathbf{x}\|^2} = \frac{\max_{\mathbf{p}}\left|\mathbf{x}^{\mathrm{H}}\mathbf{P}\mathbf{x}\right|^2}{\|\mathbf{x}\|^2} = 1 - \frac{\min_{\mathbf{p}}\left|\mathbf{x}^{\mathrm{H}}\mathbf{P}^{\perp}\mathbf{x}\right|^2}{\|\mathbf{x}\|^2} \underset{H_0}{\overset{H_1}{\gtrless}} T$$

$$\mathbf{P}^{\perp} = \mathbf{I} - \mathbf{a}\left(\mathbf{a}^{\mathrm{H}}\mathbf{a}\right)^{-1}\mathbf{a}^{\mathrm{H}} = \mathbf{I} - \mathbf{a}\mathbf{a}^{\mathrm{H}}$$

The maximization at the numerator selects the **highest peak of the beamforming** and normalizes to the data vector norm.

- A. De Maio, G. Fornaro, A. Pauciullo, Detection of Single Scatterers in Multidimensional SAR Imaging, IEEE Trans. Geosci. Remote Sens.,Vol. 47, No. 7, pp. 2284-2297, Jul. 2009

Sequential GLRT with cancellation (GLRT-C)

Estimation from the data of the direction of the first scatterer and evaluation of the coherence $L_1(\mathbf{x})$

Projection of the data in the complement orthogonal to the subspace spanned by the estimated direction

Estimation from the projected data of the direction of the second scatterer and evaluation of the coherence $L_2(\mathbf{x})$

$$L_1(\mathbf{x}) = \frac{\max_{\mathbf{p}_1} \left| \mathbf{a}^{\mathrm{H}}(\mathbf{p}_1)\mathbf{x} \right|^2}{\|\mathbf{a}\|^2 \|\mathbf{x}\|^2} = \max_{\mathbf{p}_1} \frac{\left| \mathbf{a}^{\mathrm{H}}(\mathbf{p}_1)\mathbf{x} \right|^2}{\|\mathbf{x}\|^2} = 1 - \frac{\min_{\mathbf{p}_1} \left| \mathbf{x}^{\mathrm{H}} \mathbf{P}_1^{\perp} \mathbf{x} \right|^2}{\|\mathbf{x}\|^2}$$

$$\hat{\mathbf{P}}_1^{\perp} = \mathbf{I} - \hat{\mathbf{a}}_1 \hat{\mathbf{a}}_1^{\mathrm{H}} \qquad \mathbf{x}_{\mathrm{c}} = \hat{\mathbf{P}}_1^{\perp} \mathbf{x}$$

$$\hat{\mathbf{a}}_1 = \mathbf{a}(\hat{\mathbf{p}}_1) \qquad \mathbf{a}_{2\mathrm{c}} = \hat{\mathbf{P}}_1^{\perp} \mathbf{a}_2$$

$$L_2(\mathbf{x}) = \max_{\mathbf{p}_2} \frac{\left| \mathbf{a}_{2\mathrm{c}}^{\mathrm{H}}(\mathbf{p}_2)\mathbf{x}_{\mathrm{c}} \right|^2}{\left\| \mathbf{a}_{2\mathrm{c}}(\mathbf{p}_2) \right\|^2 \|\mathbf{x}_{\mathrm{c}}\|^2}$$

Advantages: requires only one dimensional maximizations **(computational time)**

Disadvantages: **no super-resolution**

- A. Pauciullo, D. Reale, A. De Maio, G. Fornaro, Detection of Double Scatterers in SAR Tomography, IEEE Trans. Geosci. Remote Sens., Vol. 50, No. 9, pp. 3567-3586, Sept. 2012

Scheme of the GLRT-C detector

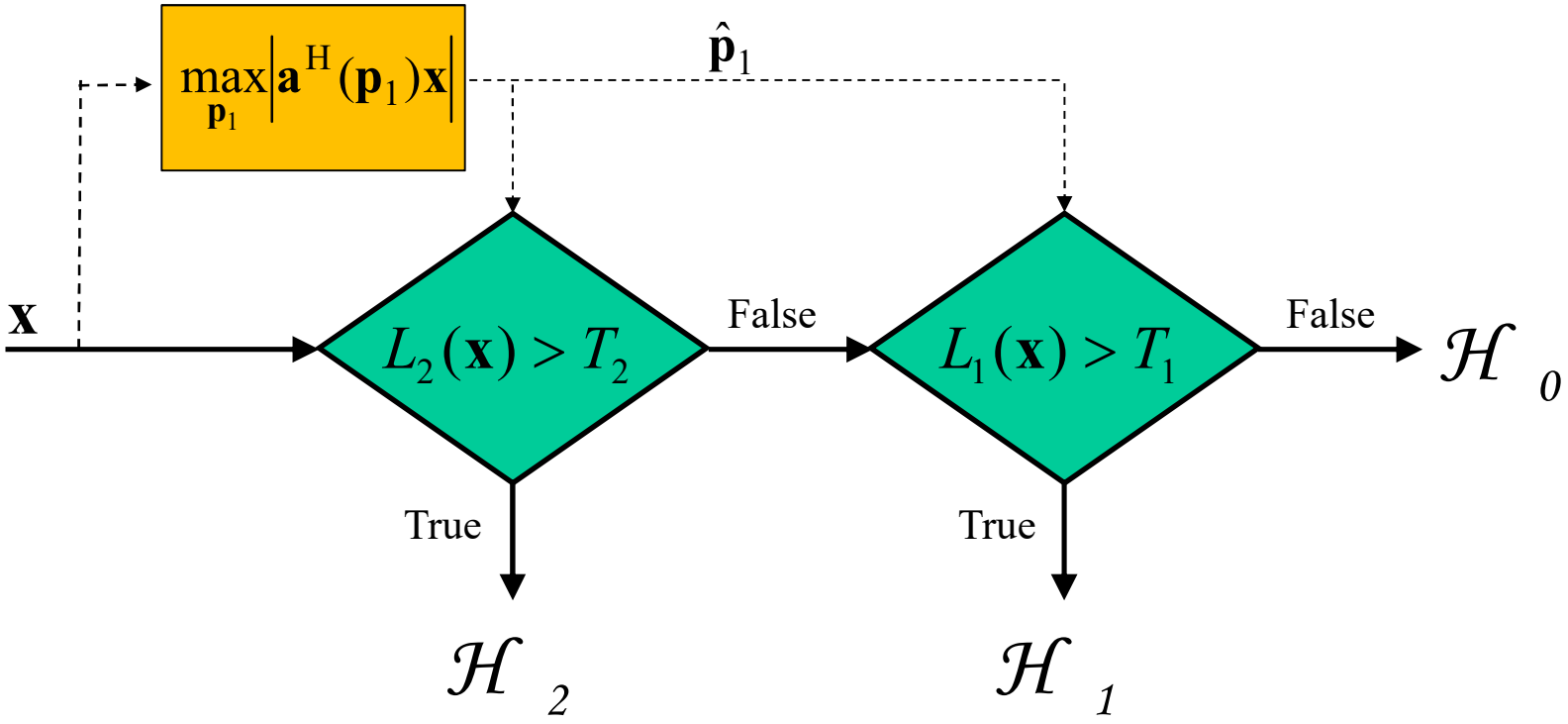

The thresholds T_1 and T_2 are set based on the fixed values of PFA, on the first and on the second scatterers

sup-GLRT: an advance over the GLRT-C

$$\mathcal{H}_0: \quad \mathbf{x} = \mathbf{w}$$
$$\mathcal{H}_1: \quad \mathbf{x} = \mathbf{a}_1\gamma_1 + \mathbf{w}$$
$$\mathcal{H}_2: \quad \mathbf{x} = \mathbf{a}_1\gamma_1 + \mathbf{a}_2\gamma_2 + \mathbf{w}$$

ML estimation

$$\arg\min_{\mathbf{p}_1,\mathbf{p}_2}\left|\mathbf{x}^{\mathrm{H}}\mathbf{P}^{\perp}(\mathbf{p}_1,\mathbf{p}_2)\mathbf{x}\right|^2 = \arg\max_{\mathbf{p}_1,\mathbf{p}_2}\left|\mathbf{x}^{\mathrm{H}}\mathbf{P}(\mathbf{p}_1,\mathbf{p}_2)\mathbf{x}\right|^2$$

$$\arg\min_{\mathbf{p}_1}\left|\mathbf{x}^{\mathrm{H}}\mathbf{P}^{\perp}(\mathbf{p}_1)\mathbf{x}\right|^2 = \arg\max_{\mathbf{p}_1}\left|\mathbf{x}^{\mathrm{H}}\mathbf{P}(\mathbf{p}_1)\mathbf{x}\right|^2$$

sup-GLRT

$$g_1 = 1 - \frac{\min_{\mathbf{p}_1,\mathbf{p}_2}\left|\mathbf{x}^{\mathrm{H}}\mathbf{P}^{\perp}(\mathbf{p}_1,\mathbf{p}_2)\mathbf{x}\right|^2}{\mathbf{x}^{\mathrm{H}}\mathbf{x}}$$

$$g_2 = 1 - \frac{\min_{\mathbf{p}_1,\mathbf{p}_2}\left|\mathbf{x}^{\mathrm{H}}\mathbf{P}^{\perp}(\mathbf{p}_1,\mathbf{p}_2)\mathbf{x}\right|^2}{\min_{\mathbf{p}_1}\left|\mathbf{x}^{\mathrm{H}}\mathbf{P}^{\perp}(\mathbf{p}_1)\mathbf{x}\right|^2}$$

$$g_1 \underset{H_0}{\overset{\overline{H}_0}{\gtrless}} T_1 \qquad g_1 > T_1 \quad g_2 \underset{H_1}{\overset{H_2}{\gtrless}} T_2$$

Advantages: allows **super-resolution** (i.e. detection of targets below the Rayleigh resolution)

Disadvantages: **computationally demanding**

- A. Budillon, G. Schirinzi, GLRT Based on Support Estimation for Multiple Scatterers Detection in SAR Tomography, IEEE Journ. Select. Topic. Appl. Earth Observ. Remote Sens., Vol. 9, No. 3, pp. 1086-1094, March 2016

The TERRASAR-X dataset over Las Vegas

- 25 TerraSAR-X Spotlight acquisitions over the city of Las Vegas USA (from 2008. 02. 02 to 2009. 04. 06)

- Imaging Mode: HS (High Resolution Spotlight)

- Orbit Direction: Ascending
- Beam Identification: spot_042
- Orbit Number: 3522

- Incidence Angle: 35.8°
- Look Direction: Right

- Azimuth resolution: ~ 1.1 meters
- Slant Range resolution: ~ 0.6 meters

- Polarisation Mode: Single
- Polarisation: VV

Acquisition distribution of the Las Vegas dataset

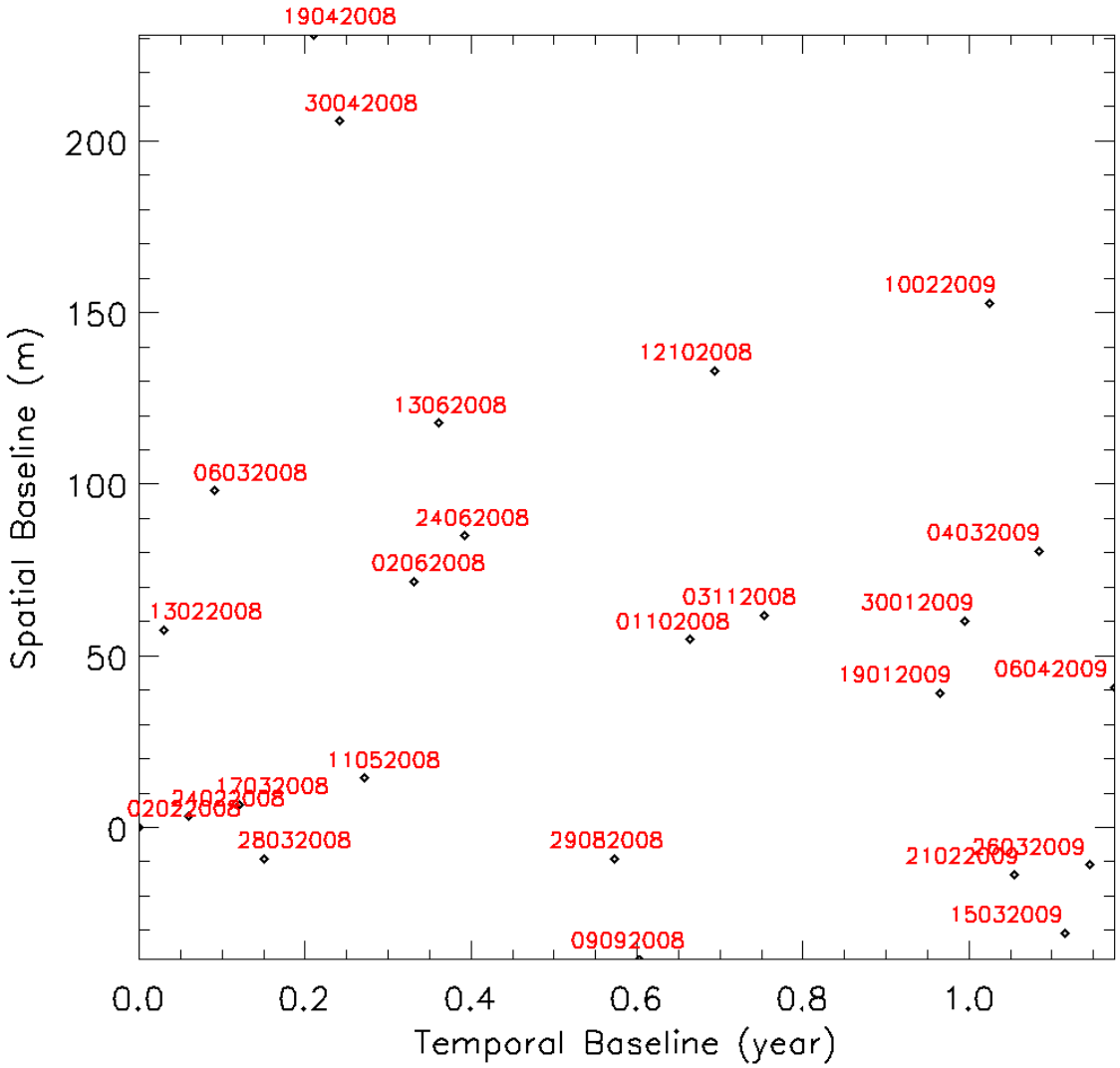

Rayleigh resolution:
40m (slant height)
27m (vertical)

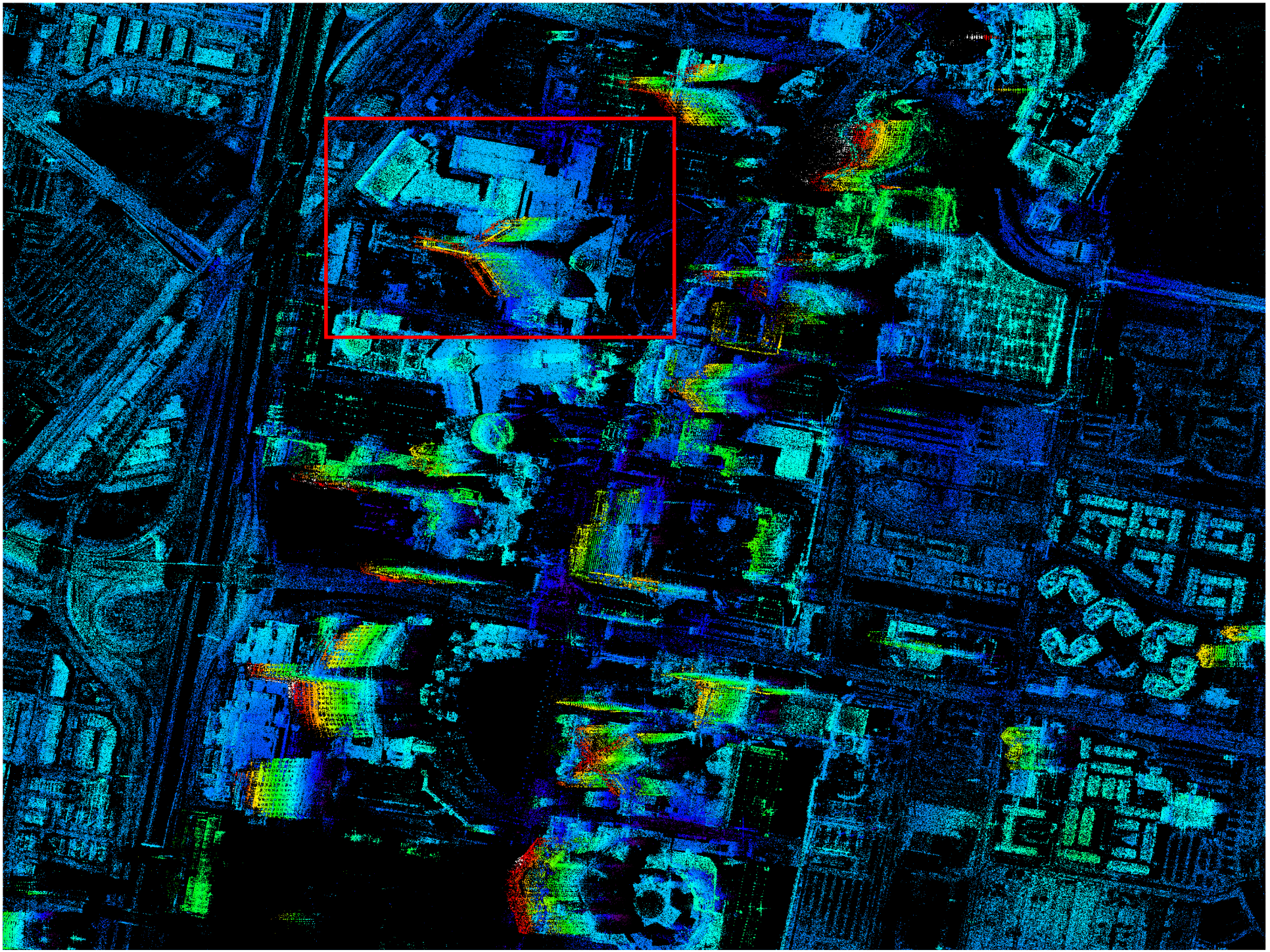

Application to high resolution data (The Mirage Hotel)

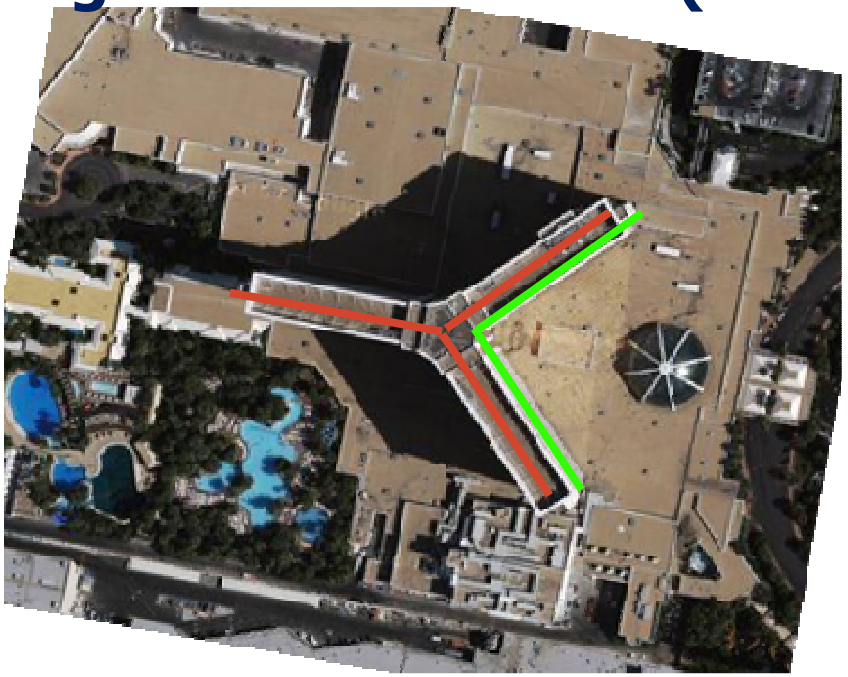

CS Detected Single Scatterers

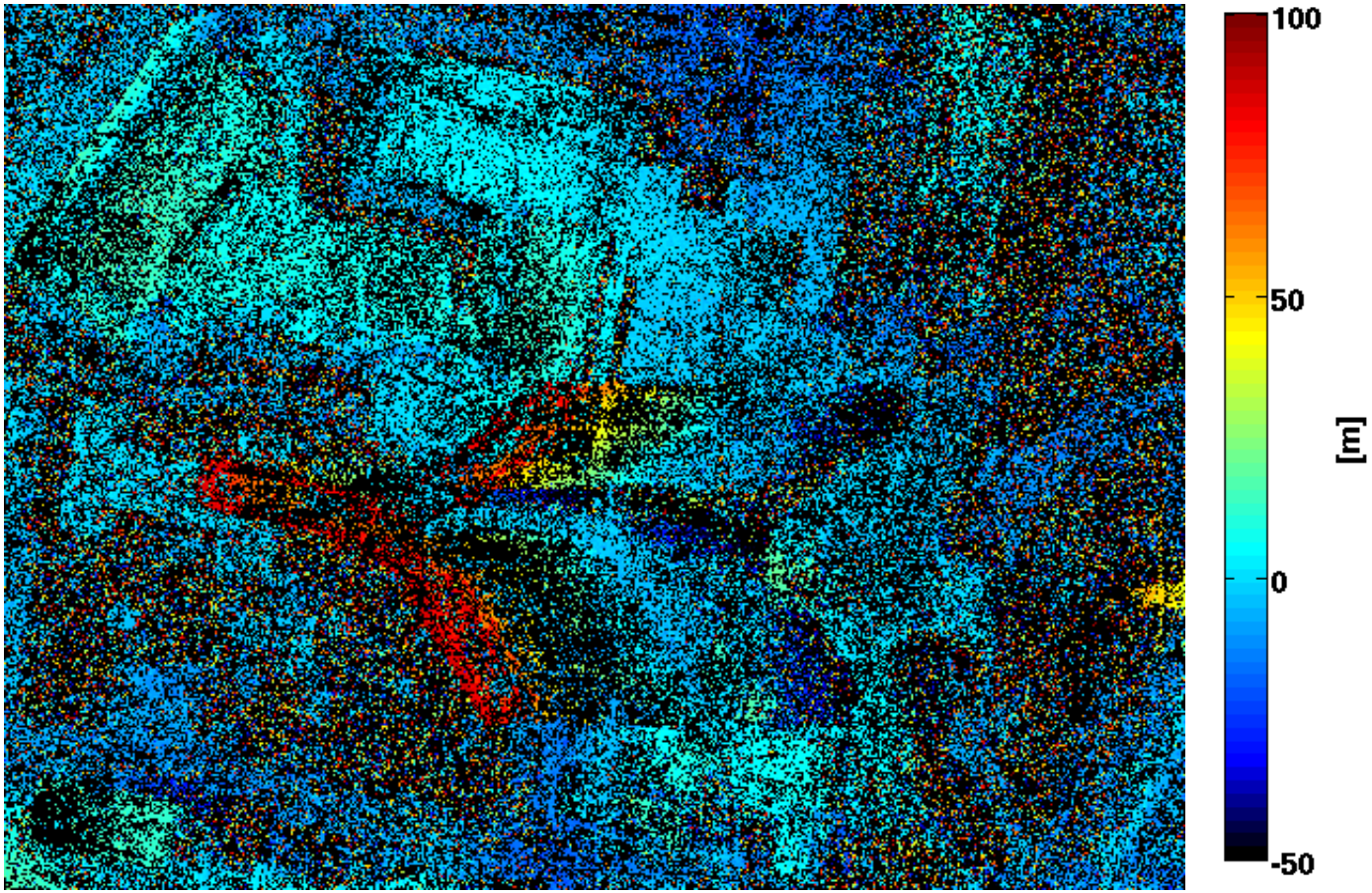

CS Detected Double Scatterers (lower)

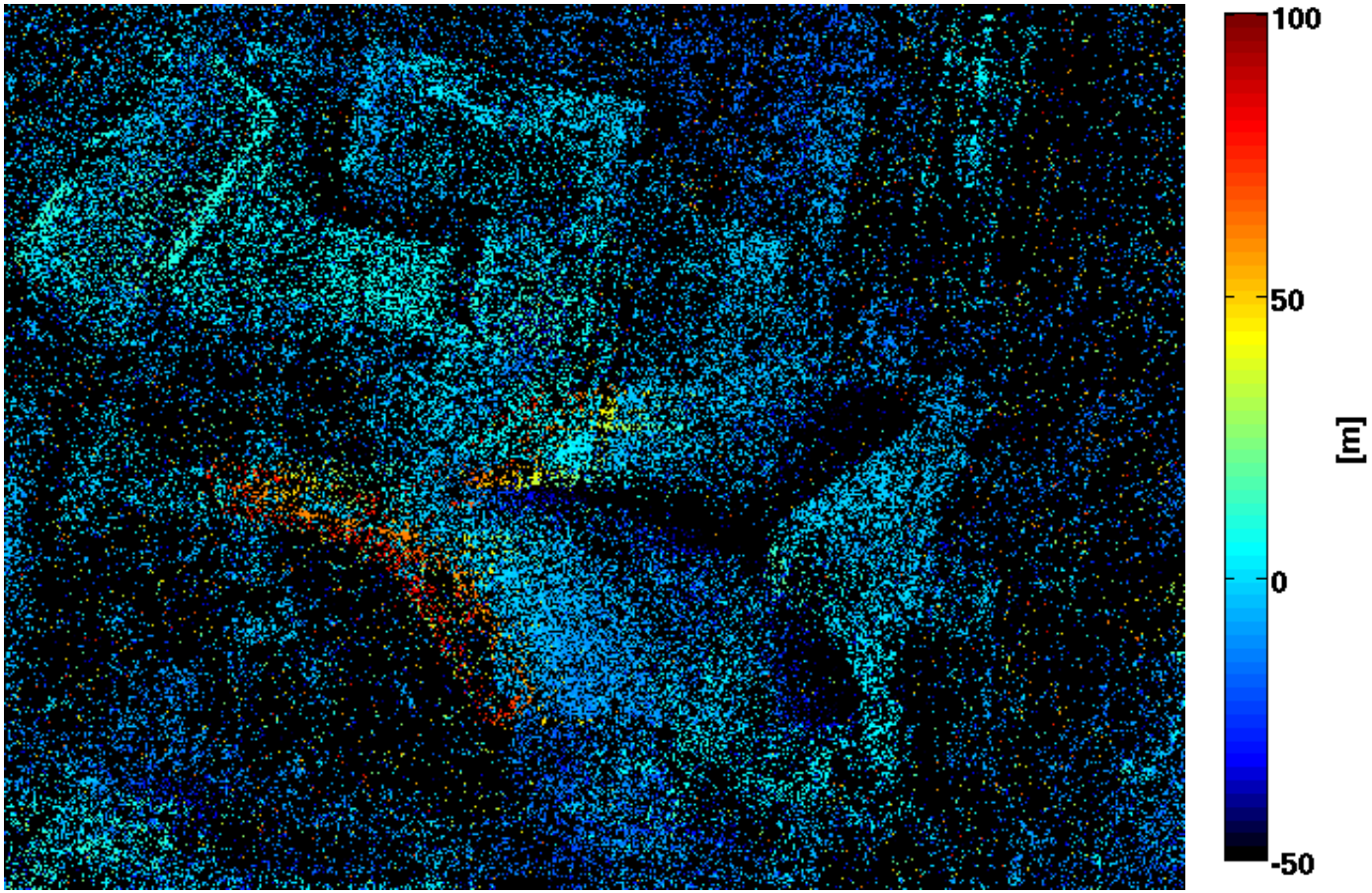

CS Detected Double Scatterers (higher)

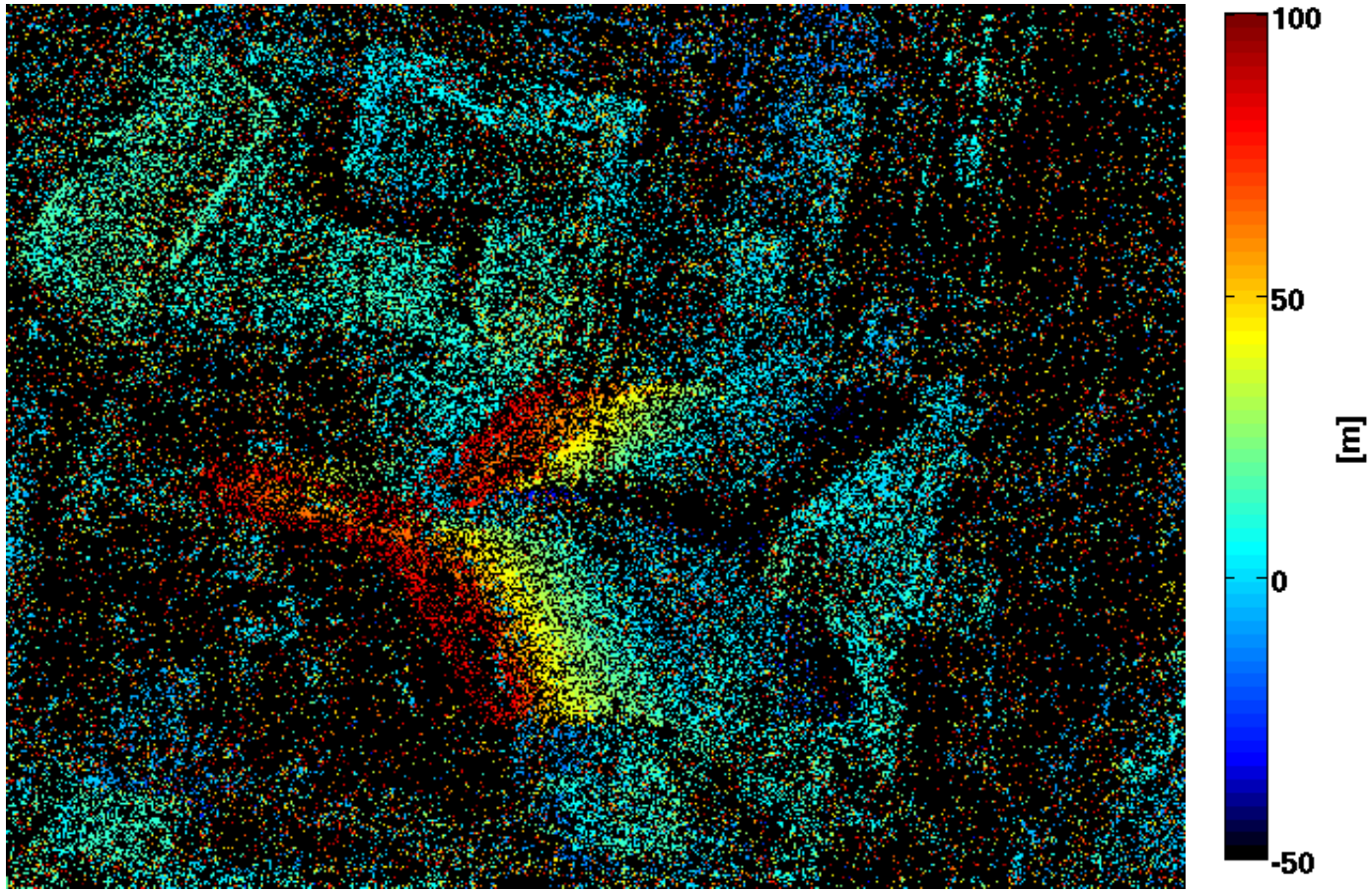

CS Detected Double Scatterers: height difference

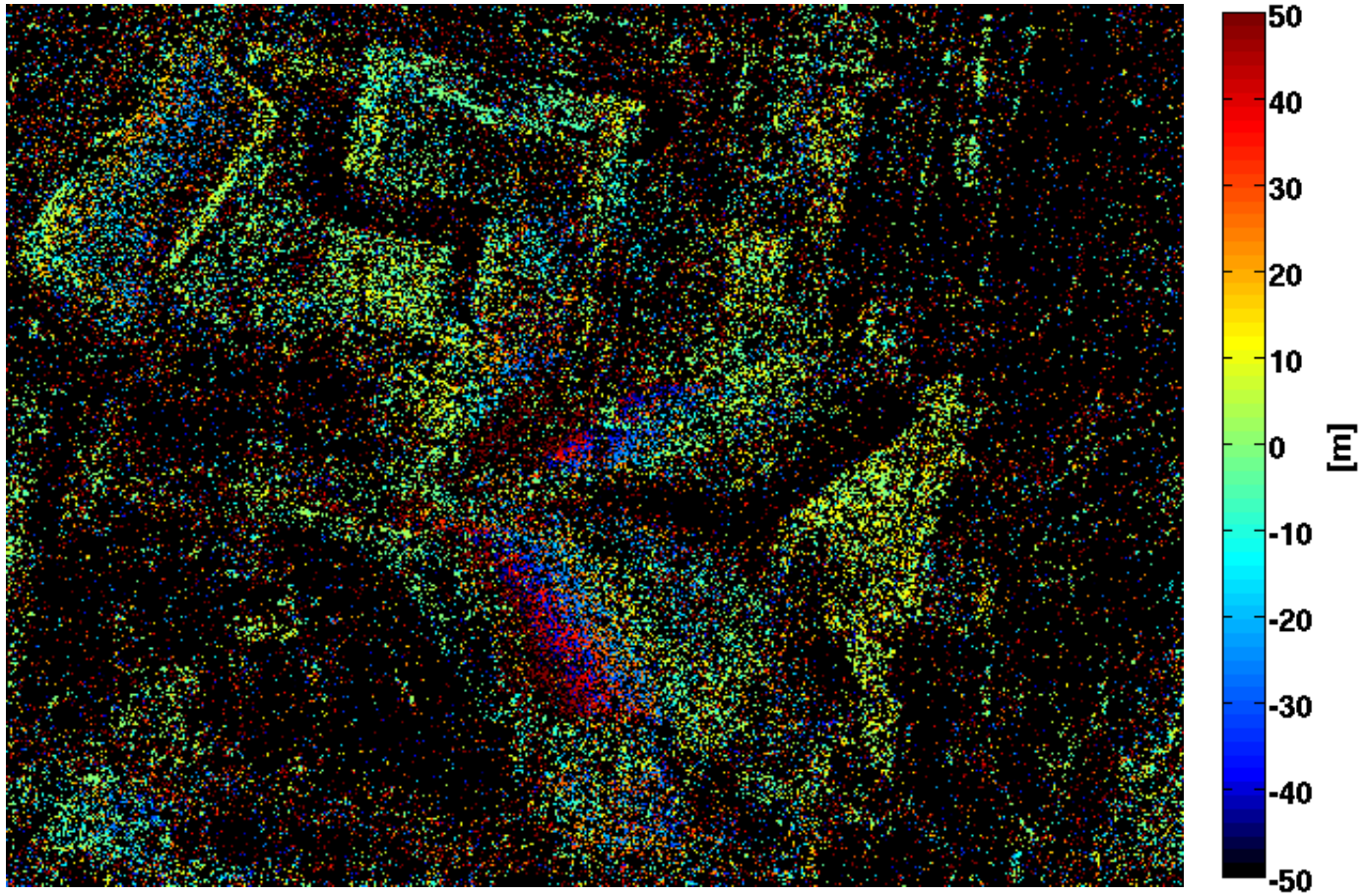

sup-GLRT Detected Single Scatterers

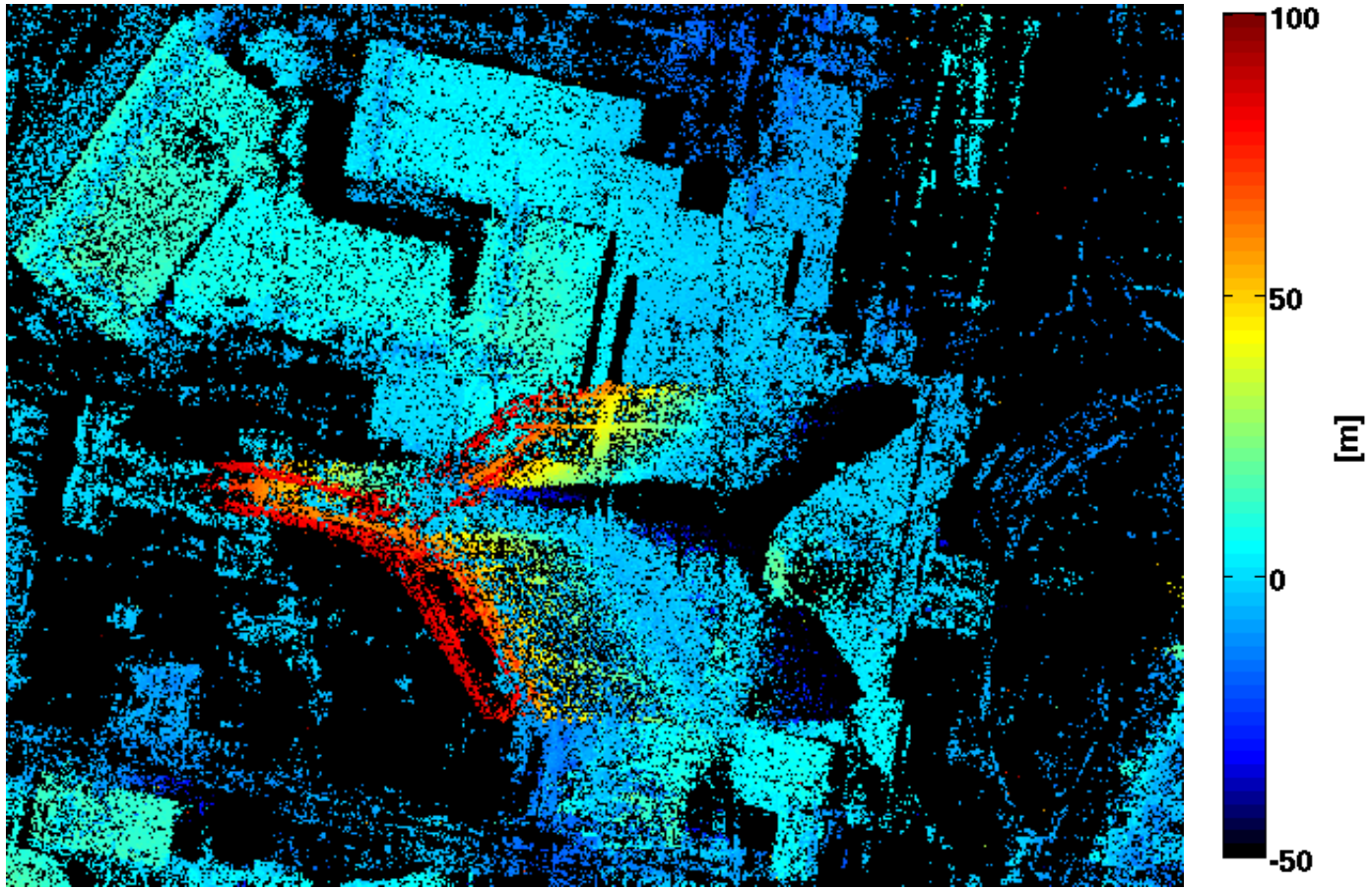

GLRT-C Detected Single Scatterers

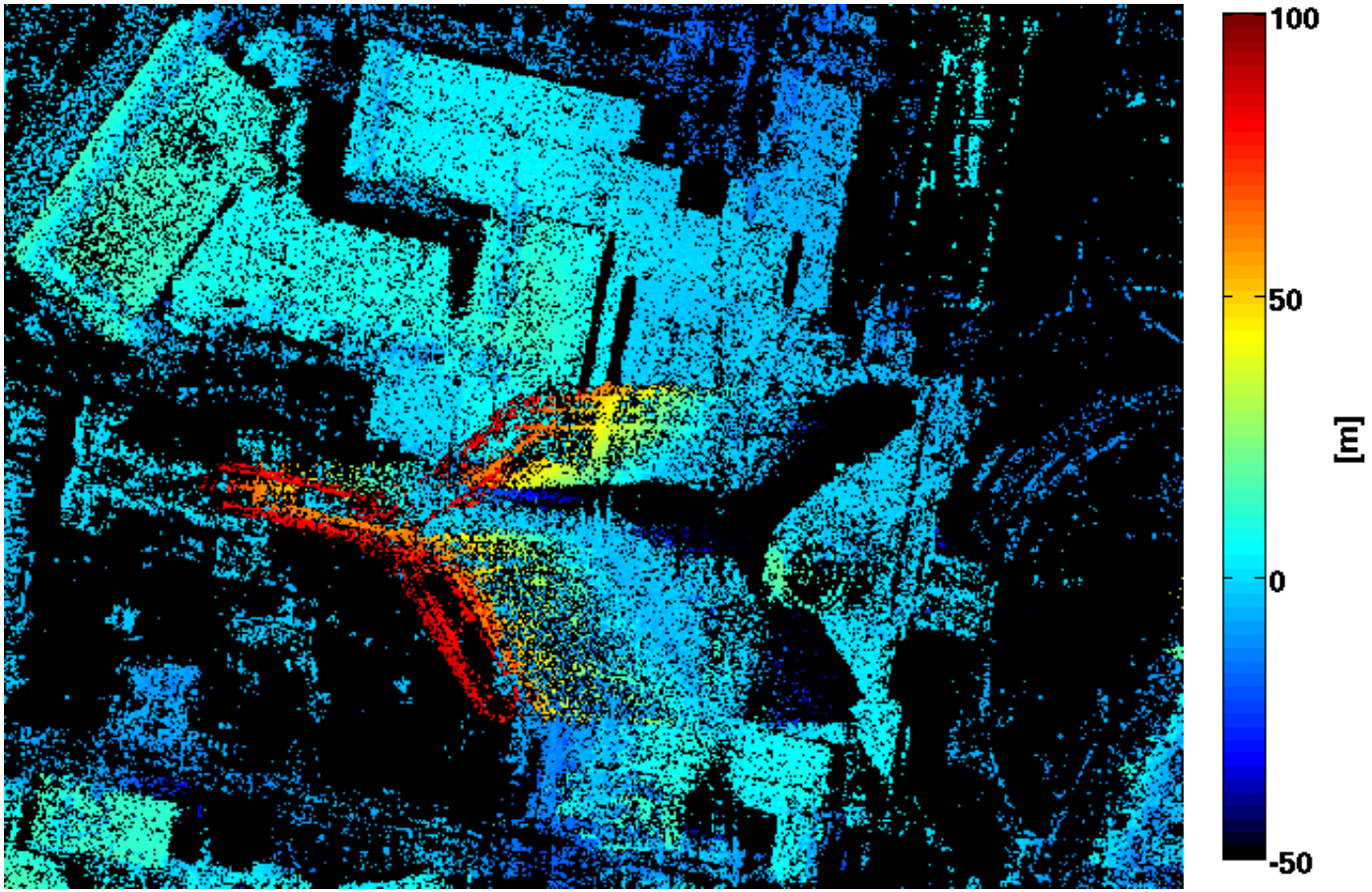

sup-GLRT Detected Double Scatterers (lower)

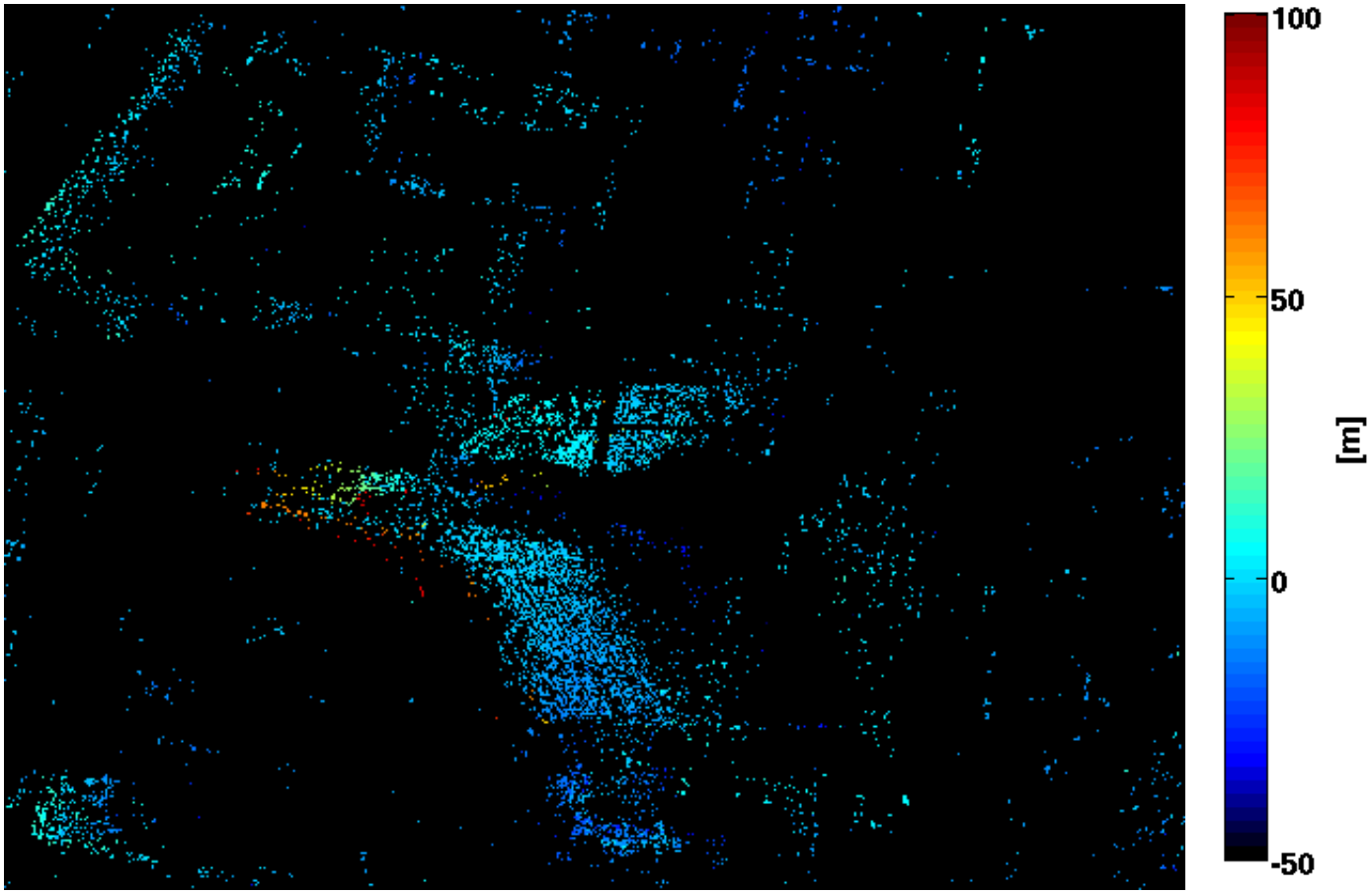

GLRT-C Detected Double Scatterers (lower)

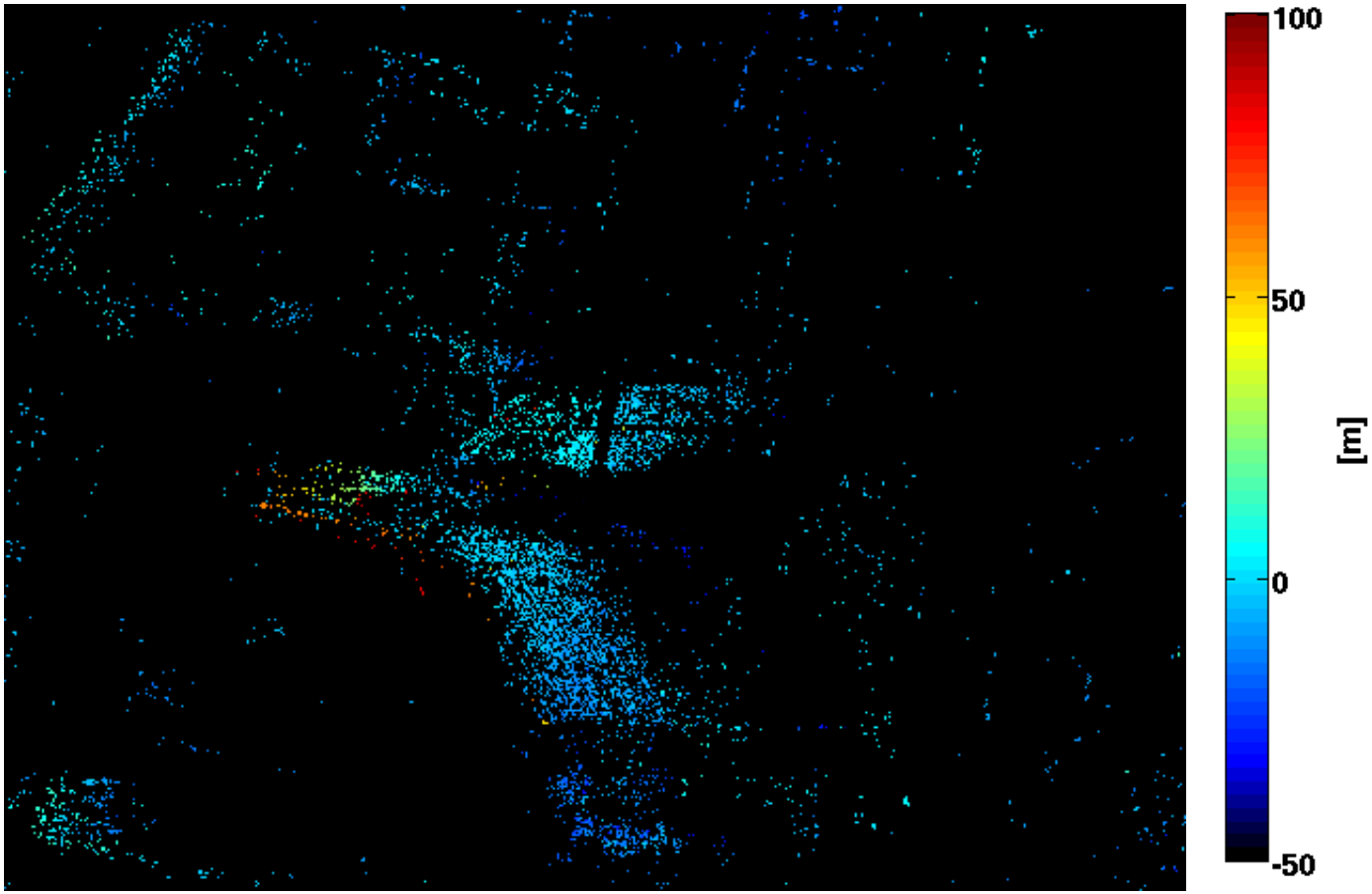

Sup-GLRT Detected Double Scatterers (higher)

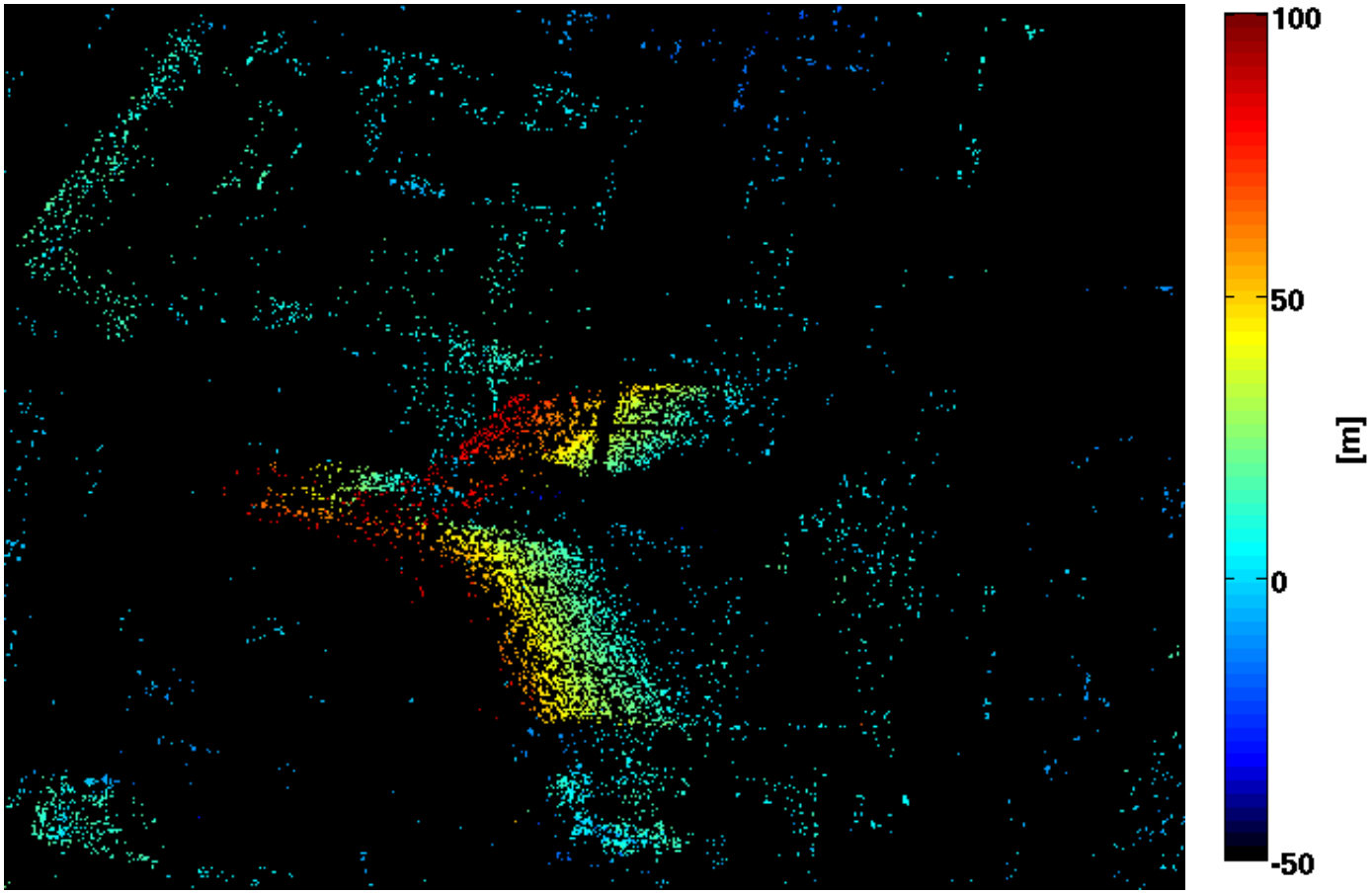

GLRT-C Detected Double Scatterers (higher)

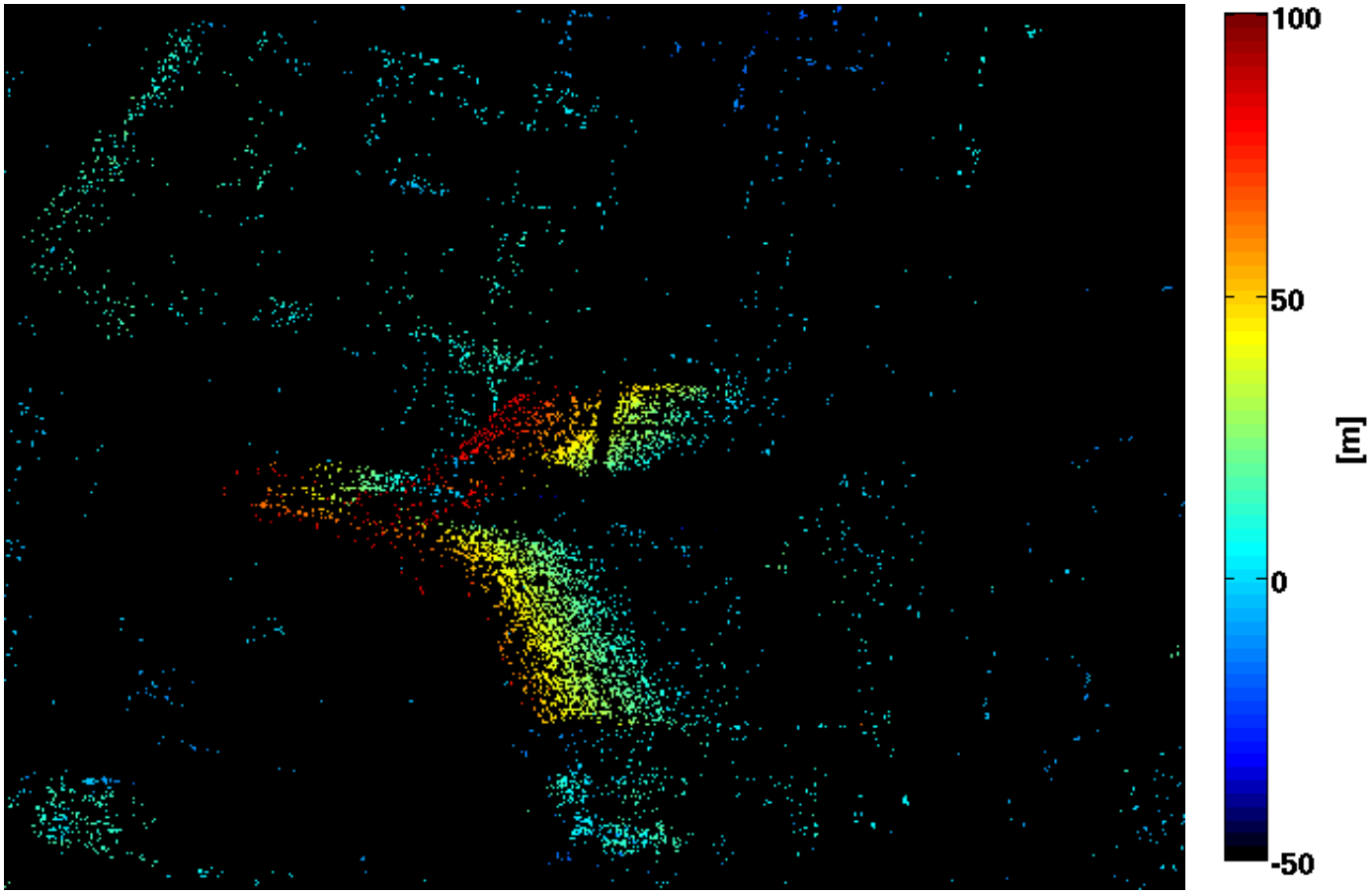

sup-GLRT Detected Double Scatterers: height difference

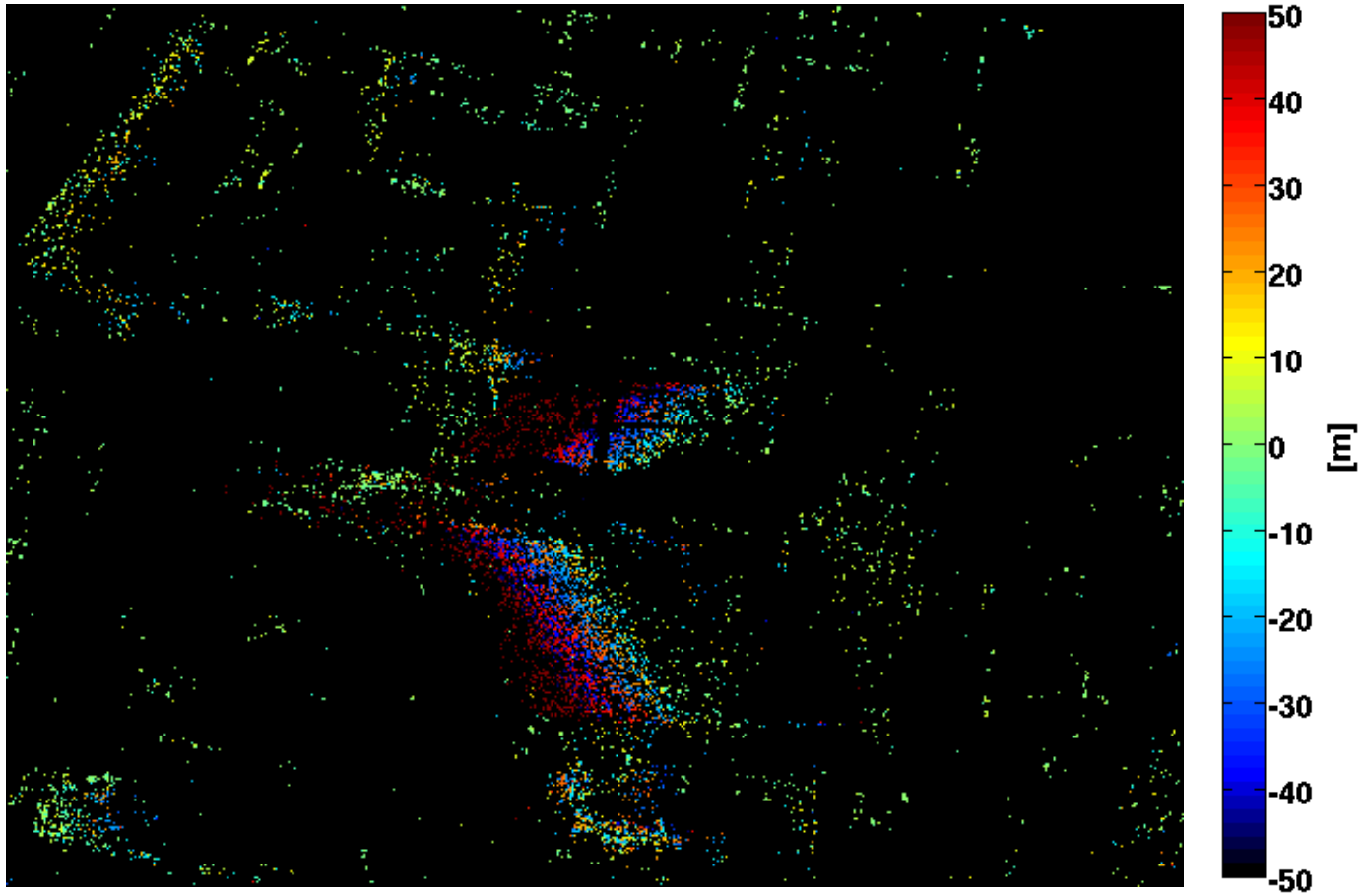

GLRT-C Detected Double Scatterers: height difference

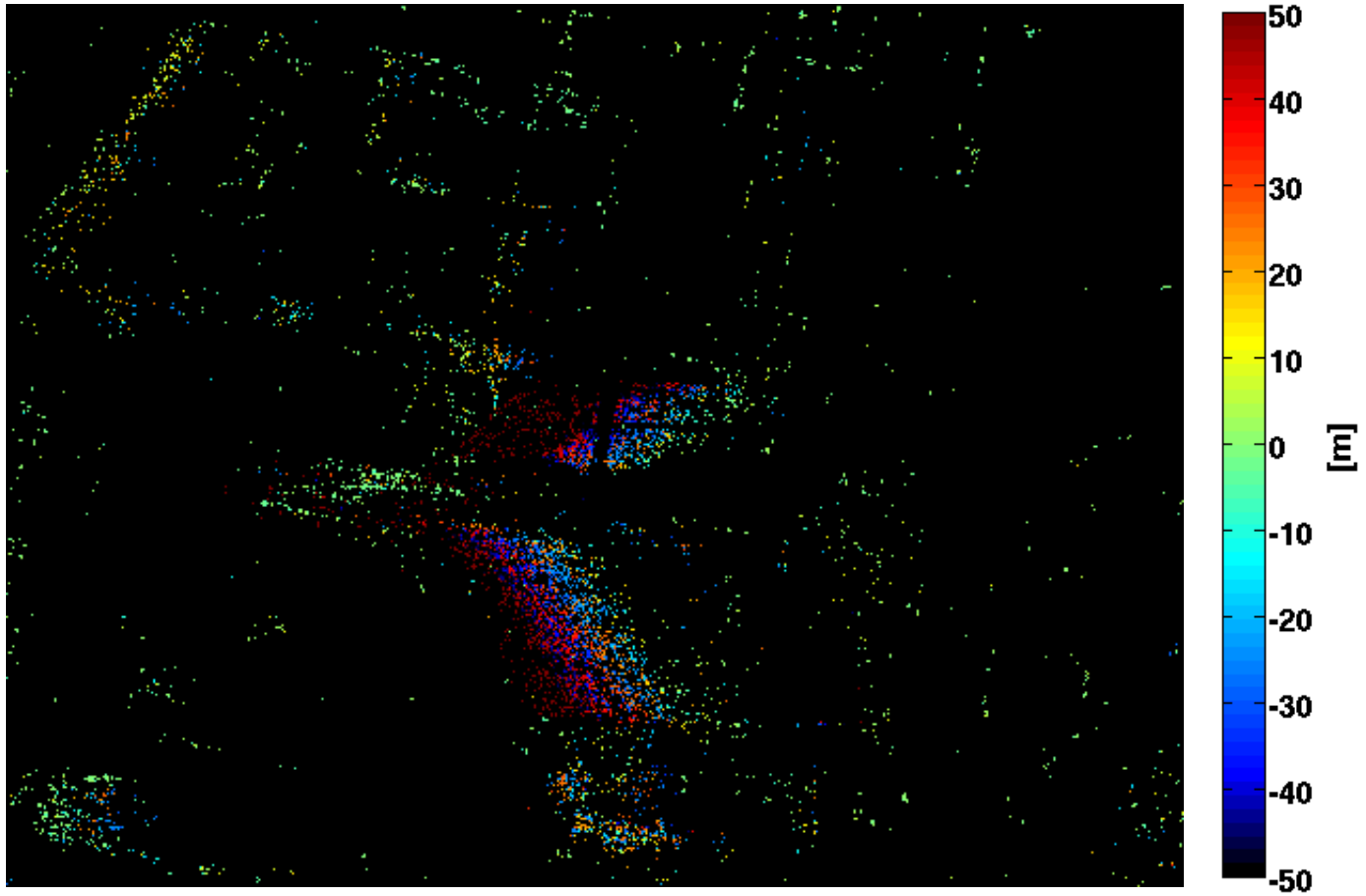

Topographic Difference Between CS and sup-GLRT

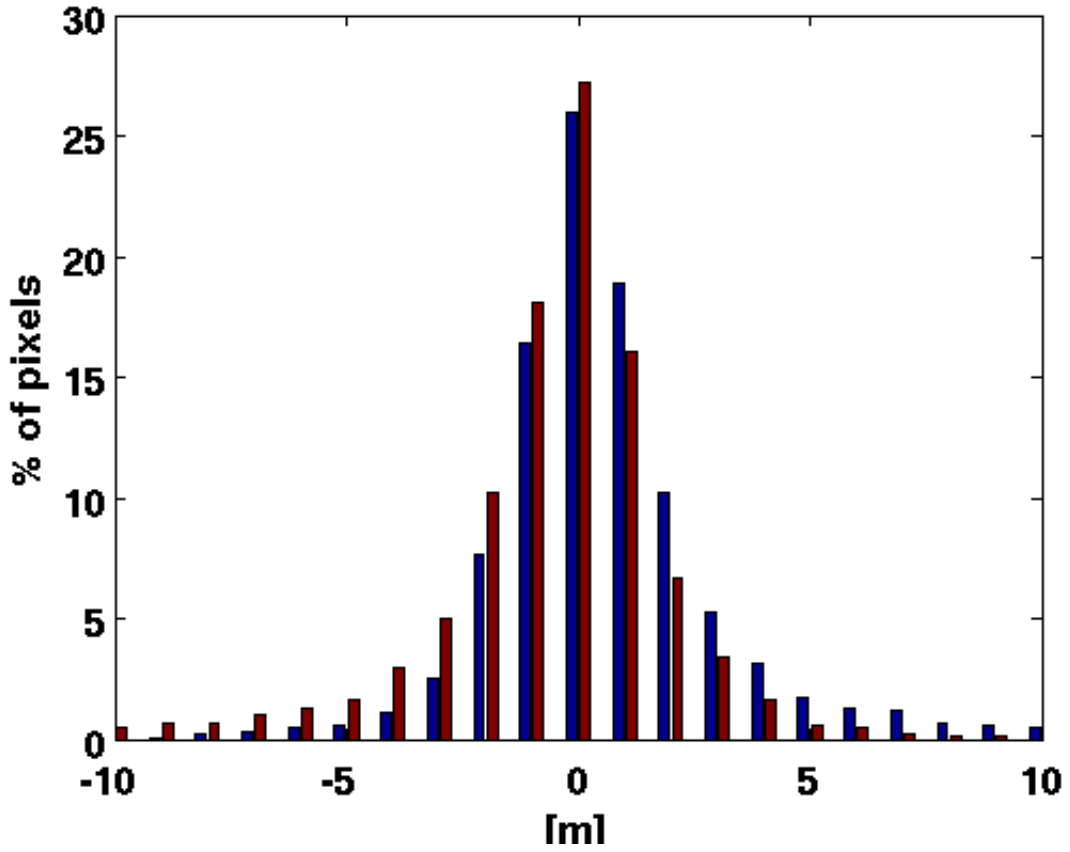

Histogram of the difference between the height of double scatterers estimated by CS and sup-GLRT (mask of points detected by sup-GLRT)

Deformation Mean Velocity Difference between CS and sup-GLRT

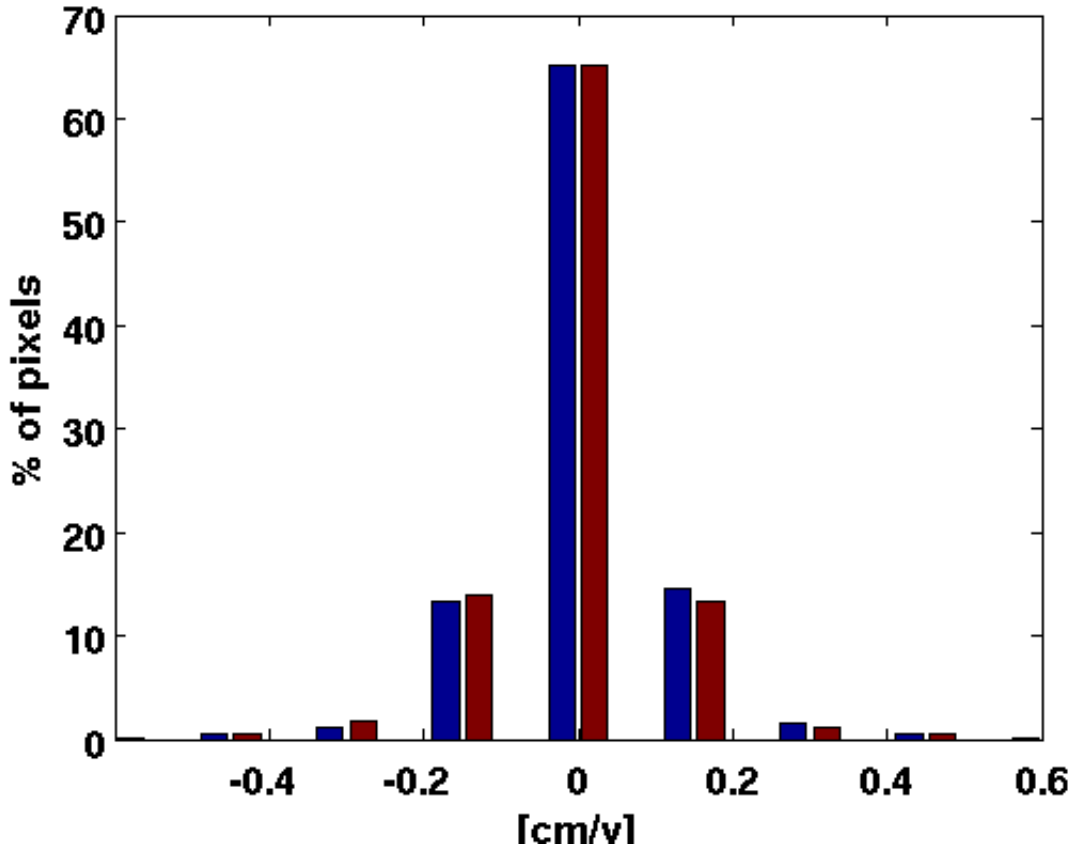

Histogram of the difference between the deformation mean velocity of double scatterers estimated by CS and sup-GLRT (mask of points detected by sup-GLRT)

CS Post Detection Single Scatterers

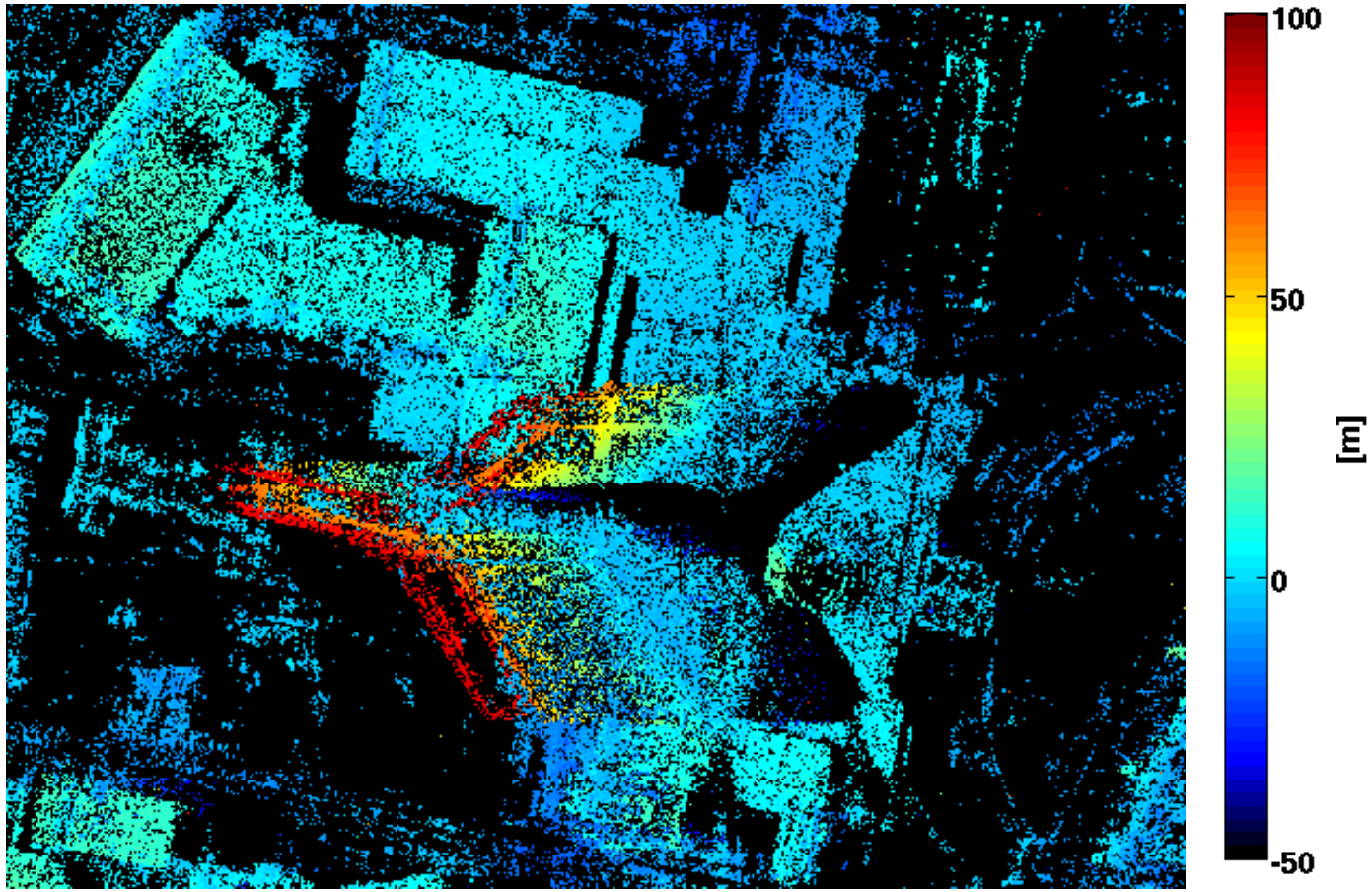

Sup-GLRT Single Scatterers

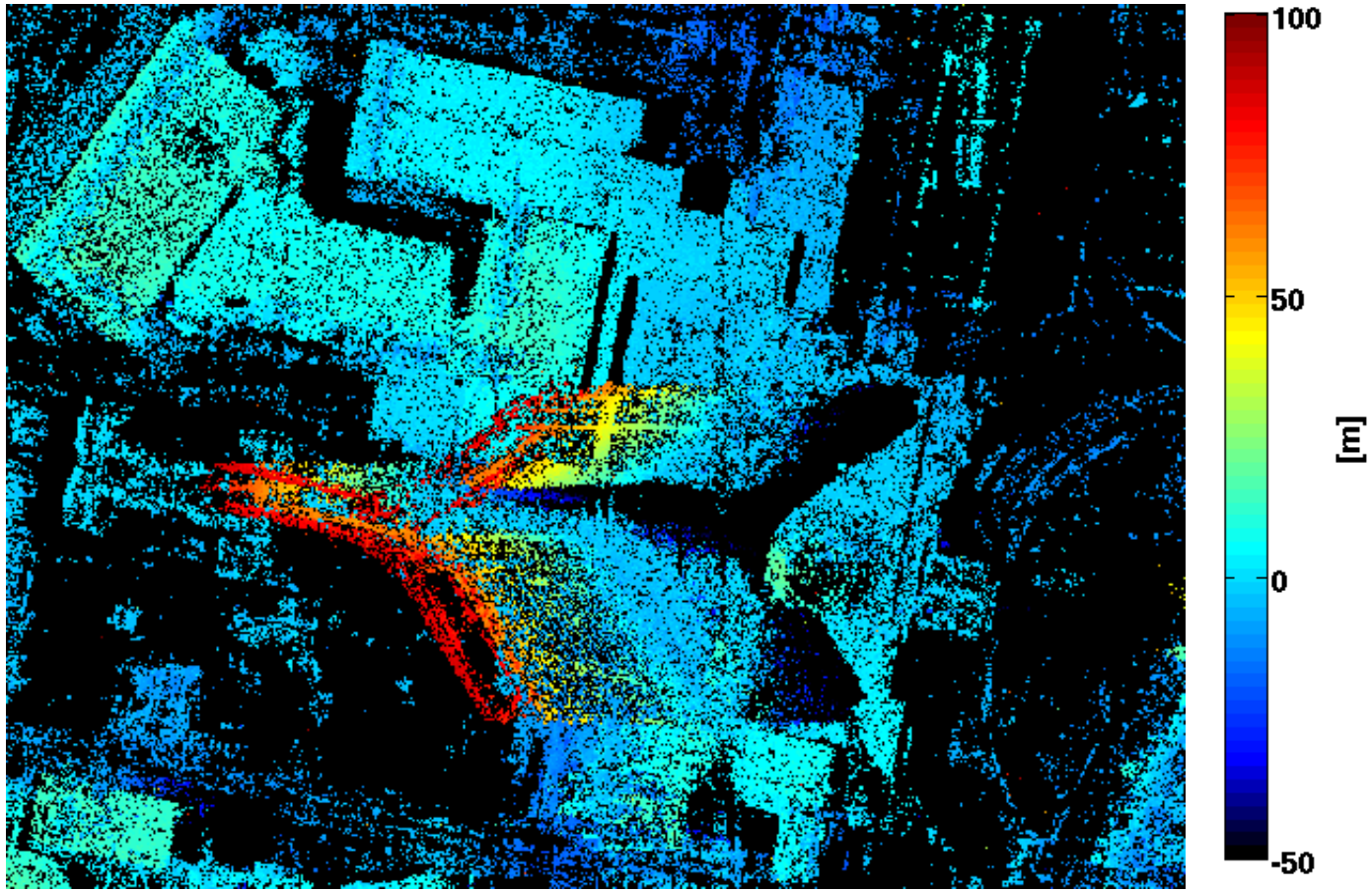

CS Post Detected Double Scatterers (lower)

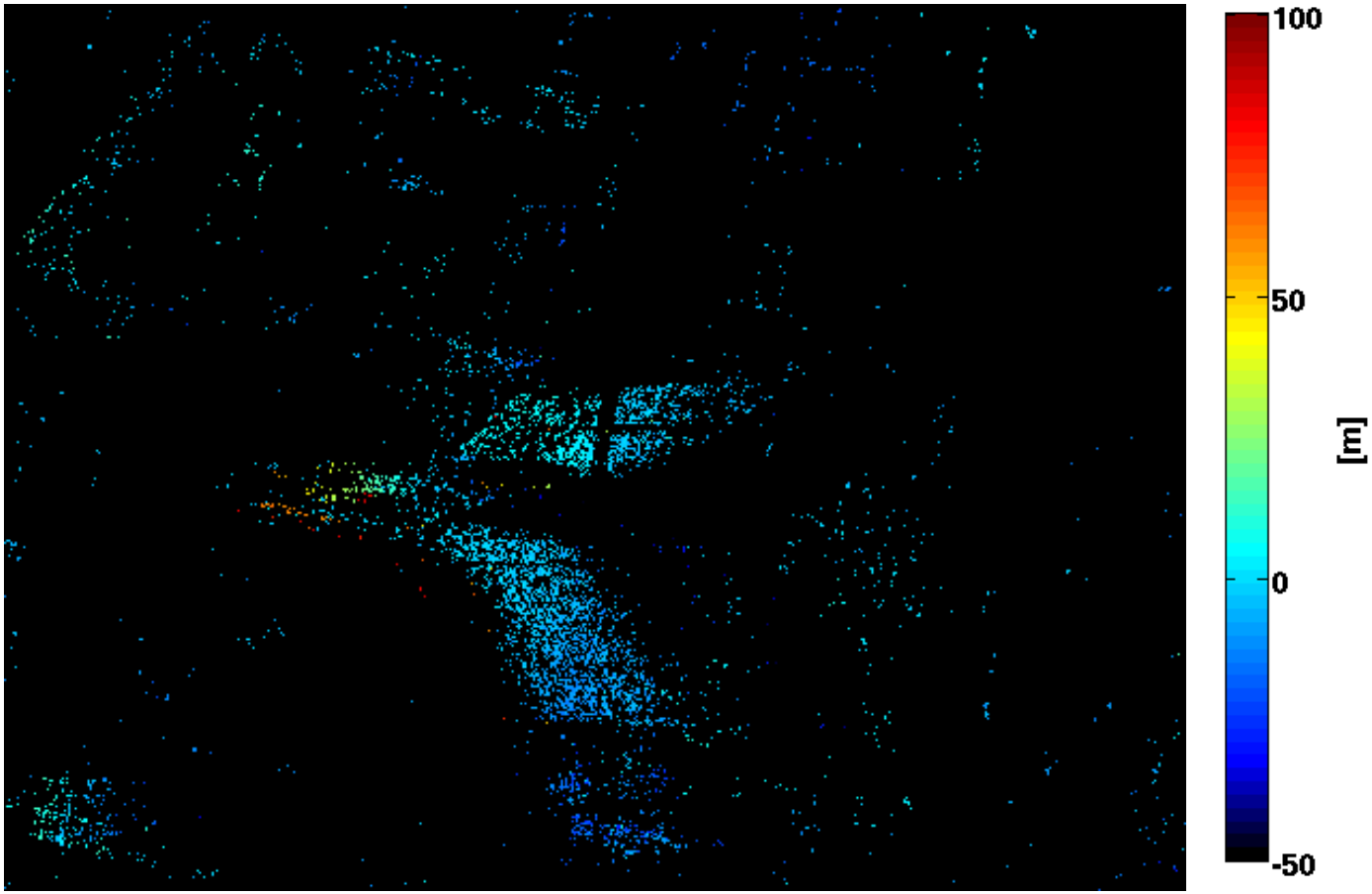

Sup-GLRT Double Scatterers (lower)

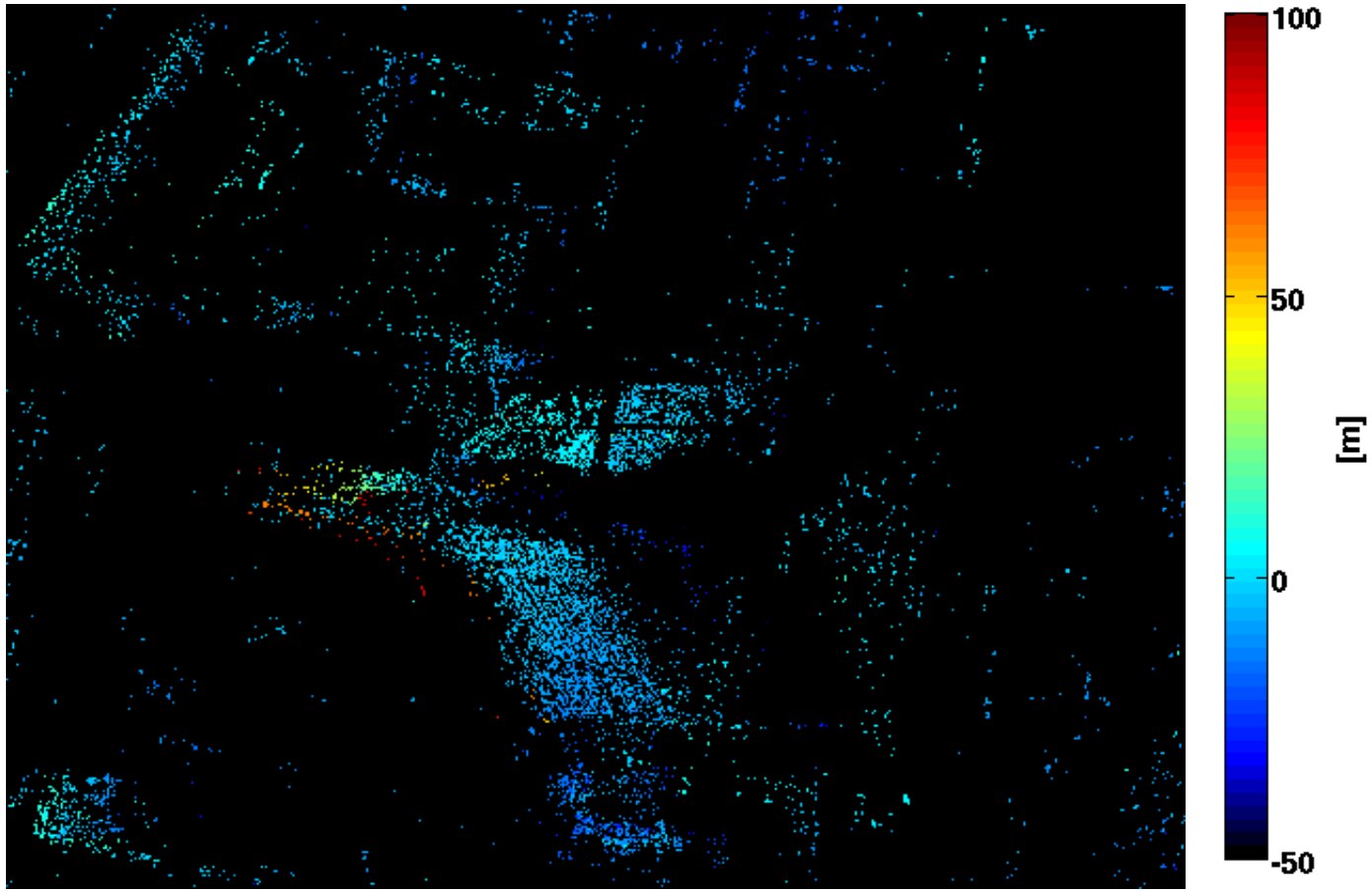

CS Post Detected Double Scatterers (higher)

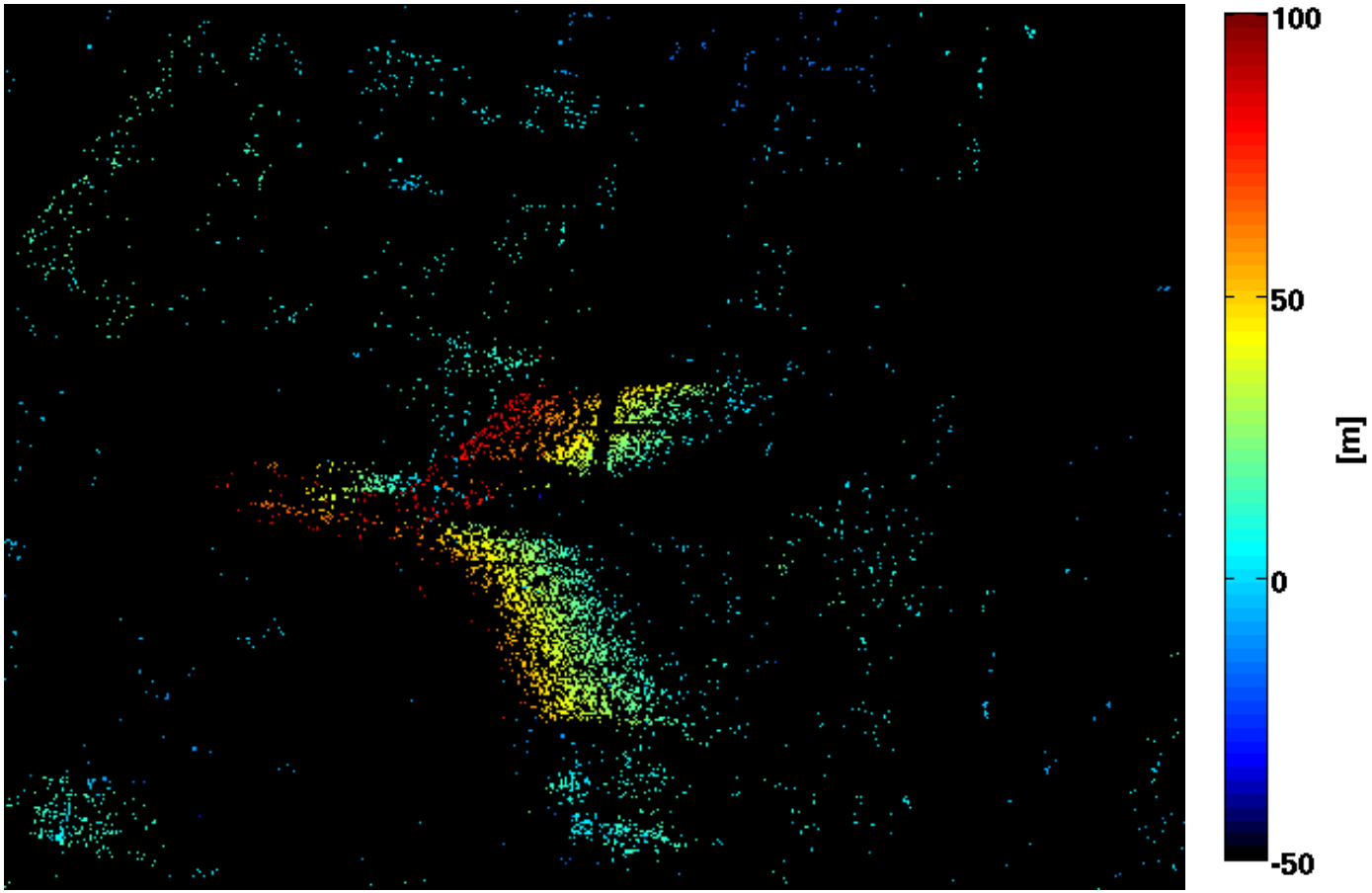

Sup-GLRT Double Scatterers (higher)

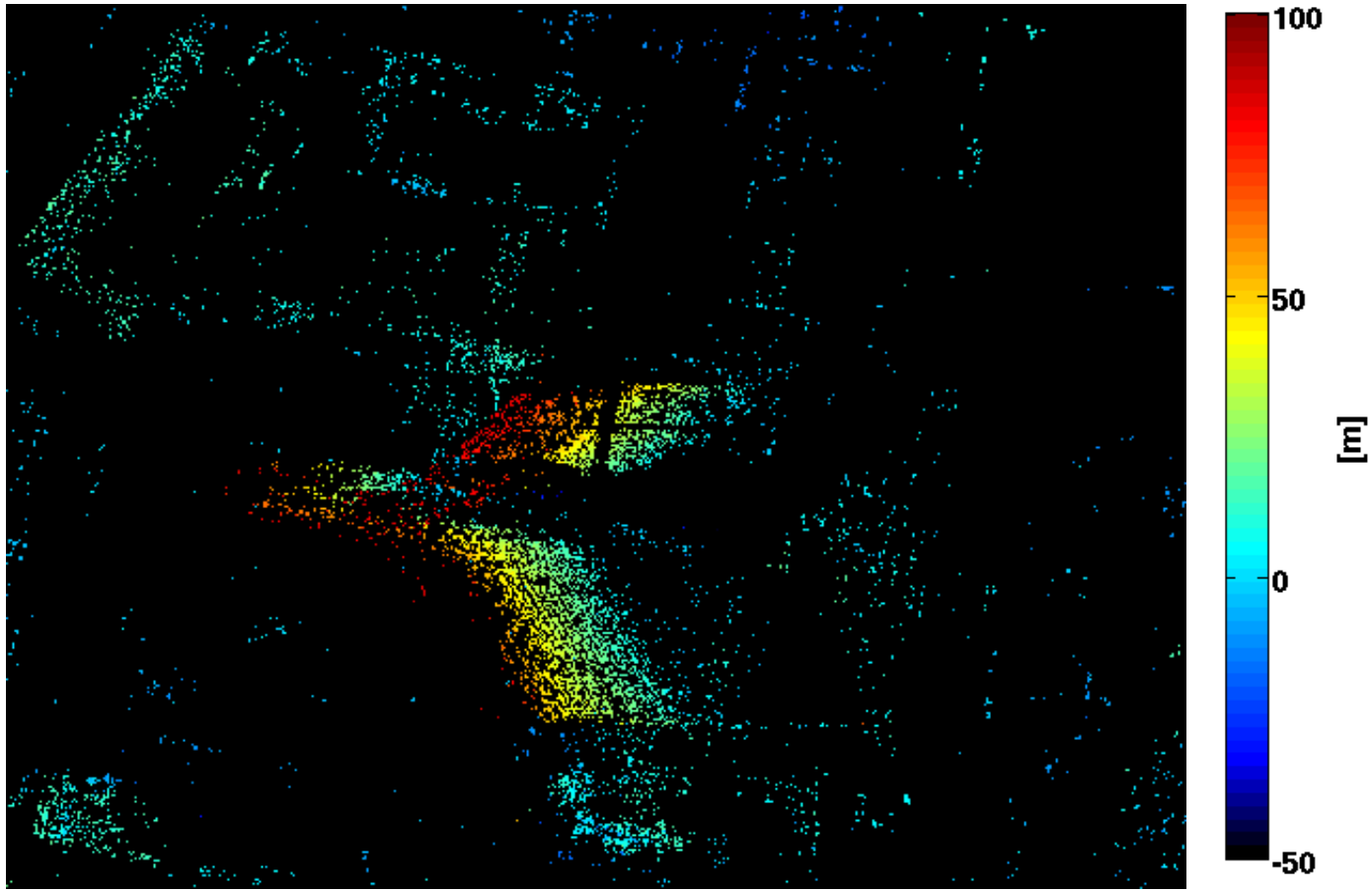

Conclusions and future works

SAR Tomography allows implementing a **radar scanner** from the space to reconstruct **3D point clouds** and monitor deformations.

Next generation VHR sensors (COSMO-SkyMED II Generation, HRWS) will allow further improving this technology for **application to urban area and critical infrastructure monitoring.**

Super-resolution in SAR tomography allows achieving improvements in the generation of 3D point clouds.

An open issue is the **coupling between the reliability of the reconstruction and the computational performances**. To this end a key point seems to be associated with the "**assimilation"** of proper detection schemes within computationally efficient L1 methods.

THANK YOU DANKE